

## Application of ceramic insulation on high temperature instrumentation wire for turbin engines

Eric R. Kreidler\* and Vidya Praveen Bhallamudi†

Dept. of Materials Science & Engineering, The Ohio State University, Columbus, Ohio

Problems with the mineral insulated, metal sheathed lead wires used to instrument aircraft engines have become more severe at the increased operating temperatures of today's engines. To solve these problems, we have applied high purity  $Al_2O_3$  directly onto platinum wires. Three coating methods have been studied, electrophoretic deposition (EPD) from ethanol suspensions, slurry coating, and EPD from aqueous suspensions. The coatings were sintered to theoretical density at 1500-1600°C. Highly adherent, crack free, coatings were obtained by the slurry coating process. When bent, the coating cracked in localized areas, but very little of it was dislodged from the wire. The wires coated by EPD from ethanol suspensions were free of cracks after drying but after sintering, regularly spaced cracks perpendicular to the wire axis developed. These cracks allow the wire to be bent around corners while still retaining the sintered coating. The coatings obtained by EPD from aqueous suspensions contained large voids due to the gas bubbles generated by electrolysis of water. After drying, these coatings exhibited two different crack patterns. One pattern was similar to that seen in sintered coatings obtained by EPD from organic systems. The other crack pattern occurred in thin coatings and consisted of an interconnected network of longitudinal and perpendicular cracks. The latter cracking pattern is undesirable. The deposition rates of the coatings were studied as functions of the variables in the processes. Although all three coating methods were sufficiently rapid to serve as the basis for a commercial process, aqueous EPD coatings are not recommended for this application. The electrical resistivity of the sintered coatings was studied as a function of temperature from 800 to 1050°C. The resistivities of the coatings at 800°C were  $3.4-7.5 \times 10^8 \Omega\text{-cm}$ , depending upon coating type.

**Key words:** coatings, electrophoretic deposition, alumina, slurry coating, resistivity, cracking patterns in coatings, electrical insulation, high temperature wires.

### Introduction

The efficiency and performance of jet aircraft improves as the engine operating temperature increases. Consequently, there has been a steady trend to increase the operating temperature of turbine engines. In the design and development stage, engines may be equipped with dozens of sensors including, thermocouples, strain gauges, and blade tip clearance detectors, to monitor conditions at critical points in the design. The signals from these sensors are led out of the engine through mineral insulated metal sheathed wires. These wires have a central metal conductor surrounded by particulate insulation, which is held in place by an outer metal sheath. The insulating materials are usually MgO or  $Al_2O_3$ , of mineral origin, and are not very pure. The wires are produced in various sizes by conventional wire drawing methods, and during this operation the insulation may be further contaminated by abrasion of material from the metal conductor and the sheath.

Engineers, who are responsible for engine instrumentation, estimate that up to 90% of the sensor failures can be traced to problems with the lead wires. At the high operating temperatures ( $>800^\circ\text{C}$ ) of engines currently under development, sensor failures have become excessive, and attention has been focused on lead wire failures and other instrumentation concerns through PIWG\*. Lead wires fail for several reasons. The insulation may become electrically conducting at high temperatures or it may be dislodged due to intense acoustic vibrations. The latter problem is most likely to occur at sharp bends in the wire. In either case the result is an electrical short between the conductor and the sheath.

The failures caused by high temperature conductivity of the MgO or  $Al_2O_3$ , used in mineral insulated wires, must be due to contamination by impurities, either present in the raw materials or picked up during wire manufacture. This must be the case because pure  $Al_2O_3$  and MgO have very high resistivity even at high temperatures. The resistivity of polycrystalline  $Al_2O_3$  at  $1000^\circ\text{C}$  is  $1.78 \times 10^7 \Omega\text{-cm}$  and that of MgO is  $1.17 \times 10^7 \Omega\text{-cm}$  [1]. These values are more than adequate for use in lead wires. Dislodgment of insul-

\*Corresponding author:

Tel : +614-392-6754

Fax: +614-392-1537

E-mail: kreidler.1@osu.edu

†At the time this work was done he was a candidate for the Master of Science Degree.

\*The Propulsion Instrumentation Working Group, organized by the Ohio Aerospace Institute, has members from NASA and all of the major producers of aircraft turbine engines in the United States.

**Table 1.** Identification and specifications for the alumina powders used in this work

Alumina code	Product code*	Particle Size ( $\mu\text{m}$ )	Specific Surface ( $\text{m}^2/\text{gm}$ )	Total impurity content** (ppm)
A	XPC-SP/LS DBM	0.23	20.3	81
B	RC-SP DBM No MgO	0.36	8.42	173
C	XPC-SP BM (No MgO)	3.6	5.53	109
D	RC-SP DBM	0.38	9.33	148
E	CR-30	0.05	25	130
F	RC-SPF-DBM No MgO	0.38	8.52	177

\*All powders (except E) were supplied by Malakoff Industries Inc. a division of Reynolds Metals Company. Alumina E was supplied by Baikowski International Corporation.

\*\*As metal oxides. The major impurities were  $\text{SiO}_2$ ,  $\text{Na}_2\text{O}$ ,  $\text{K}_2\text{O}$ ,  $\text{CaO}$ , and  $\text{Fe}_2\text{O}_3$ .

ation by mechanical vibrations is exacerbated by the fact that the insulation is present as a packed powder layer. Applying high purity insulation directly to the conductor wire and then sintering it in place to form a dense ceramic coating, could eliminate both problems. However, for this approach to work, several conditions must be met. The insulation must not become chemically contaminated during manufacture of the wire. The insulation must not react with the conductor wire during sintering. The conductor must not oxidize in air at high temperatures. The sintered insulation must strongly adhere to the wire, so that when the wire is bent very little insulation is lost. Any cracks or openings in the sintered insulation must be so small that metal to metal contact is impossible either between adjacent wires or between wires and engine components. To be used in an engine, the wire must be flexible and have a small diameter *i.e.* a pair of wires must have a combined diameter  $<0.060$  inch.

To meet the list of requirements, we chose high purity alumina as the insulating material and platinum or platinum-rhodium alloys as the conductor. This combination of materials has several advantages. The thermal expansion coefficients are well matched, and this will promote good adhesion of the  $\text{Al}_2\text{O}_3$  coating to the Pt wire. The materials will not react chemically with each other at high temperatures, and the metal will not oxidize in air at engine operating temperatures. The melting points of the metals are high enough to allow the alumina coatings to be sintered to theoretical density. Alumina was selected because it has the highest resistivity of all oxides except BeO.

The methods used to apply the coatings were electrophoretic deposition and slurry coating. These methods can be carried out in chemically pure systems and can yield high purity coatings. Since mechanical forming operations such as wire drawing have been eliminated, the purity of the coatings can be maintained throughout the manufacturing process.

## Experimental Procedures

The alumina powders used in this work are listed in

Table 1. The particle size, specific surface, and purity varied from one powder to the next, and where necessary, coating formulations were adjusted to take account of these differences. In general, the chemical purity was very high and total metallic impurities did not exceed 180 ppm. Substrate wires were either pure platinum or platinum-10% rhodium alloys having diameters of 5-10 mil. The wires were cleaned in an ultrasonic bath containing acetone prior to coating with alumina.

Water based suspensions for electrophoretic deposition (EPD) contained 10-40 wt.% (2.7-10.1 vol.%) alumina. Doubly distilled water was used for all preparations and an ammonium salt of polyacrylic acid<sup>†</sup> was used as the dispersant. In aqueous media the dispersant dissociates to give  $\text{R-COO}^-$  ions. These ions are absorbed onto the alumina surface and give the particles a negative charge. The dispersant was added at a rate of 0.5 mg per square meter of alumina surface. The suspensions were ball milled in 1000 ml, wide mouth, high density, polyethylene, bottles for 24-48 hours. The milling media were 1/2" alumina spheres.

The suspensions used for non-aqueous EPD were prepared with mixtures of ethanol and acetone. When pure ethanol was used, deposition was not observed at 250 Volts, the limit of our power supply<sup>‡</sup>. Addition of acetone lowered the deposition voltage, but because of its high vapor pressure, the amount of acetone was kept at or below 25% by volume. A typical suspension contained 35 wt.% alumina and 65 wt.% ethanol-acetone mixture (75 vol.% ethanol, 25 vol.% acetone). No dispersants were used in these suspensions. The suspensions were ball milled for 24 hours in polyethylene bottles.

The suspension used for slurry coating and its preparation is outlined in Table 2. This suspension was based on a tape casting formulation reported by Faber [2]. This slurry had shear thinning characteristics, and its viscosity curve extrapolated to 38,500cP at zero shear rate.

\*Rohm and Haas Company, Duramax D-3021.

†E-C Apparatus Corporation model EC 250-90.

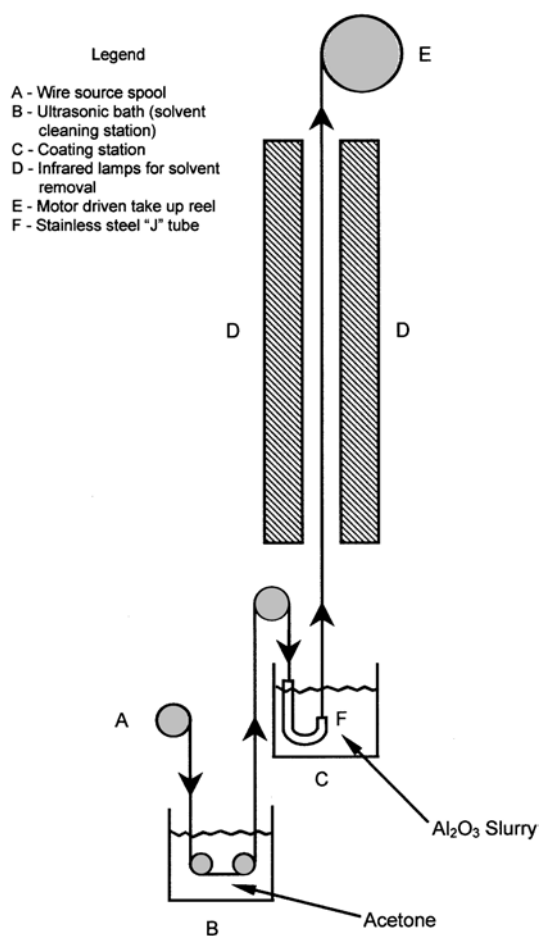
**Table 2.** Preparation of the suspension used for slurry coating

First milling	
Alumina F	100 g
Toluene (solvent)	18 ml
Methyl Ethyl Ketone (solvent)	18 ml
Defloc Z-3 (dispersant)	3 g
Santicizer (Plasticizer)	4.3 g
Ball milled for	8 hr
Second milling	
Butvar B-79 (binder)	5 g
MEK	20 ml
Toluene	20 ml
Ball milled for	24 hr

The apparatus for EPD coating consisted of a 500 ml beaker and a stand for holding the sample and counter electrode in fixed positions. The counter electrode was a 20 mil platinum wire and the samples to be coated were two-inch lengths of Pt or Pt 10% Rh wire. The distance between the electrodes was ~1.5 inches. The voltage source could be operated in either constant current or constant voltage mode, all of our coatings were made using constant current conditions. Coating thickness was controlled by limiting the deposition time and current. The slurry was agitated with a magnetic stirrer to minimize settling of the alumina particles. After the desired coating thickness was obtained, the wires were removed from the slurry and air dried while hanging in a vertical position. This was done to prevent distortion of the fragile wet coating by contact with a supporting surface.

The apparatus used for slurry coating is shown in Fig. 1. The wire was fed from a spool through an ultrasonic bath filled with acetone and then through the slurry. A stainless steel "J" tube lined with teflon was used to lead the wire under the surface of the slurry. The immersed end of the "J" tube contained a stainless steel orifice (15 mil diameter) to serve as a wire guide. The slurry container was tightly sealed except for this orifice and a 1/8" diameter exit hole for the wire. This was done to minimize solvent loss and changes in slurry viscosity. After exiting the slurry, the coated wire was passed between two 3-foot long, quartz, infrared heaters. The dried wire was taken up on a motor driven spool. We controlled the velocity of the wire through the coating machine by changing the speed of the drive motor. The coater was capable of wire speeds of 0.2 to >10.0 cm/s.

After the coatings had dried, the wires were sintered in air at 1500-1600°C, and held at the maximum temperature for 0.5-2.5 hours. To provide time for the binder to burn out, the slurry coated wires were heated at 2°C/min to 500°C, held at 500°C for one hour, and then heated to the final sintering temperature at a rate of 10°C/min. Since the EPD coatings did not contain a binder they could be heated to the sintering

**Fig. 1.** Laboratory scale wire coater.

temperature at a rate of 10°C/min with no hold at 500°C. Upon completion of sintering, the furnace was shut off and allowed to cool with the samples still inside. To minimize damage to the coatings during sintering, the samples were hung from 1/8" diameter alumina rods supported by the rim of a large alumina crucible.

The macrostructure of the samples was examined using a stereozoom microscope equipped with a video printer. The coatings were examined after drying and also after sintering, and typical coating structures were photographed. The microstructures of the coatings were examined with a Philips XL-30 FEG scanning electron microscope. To prevent charging, the samples were coated with a thin film of carbon. Thickness measurements of the coatings were obtained by measurements taken on micrographs, having known magnification.

The electrical resistance through the thickness of the coatings was measured in one of two ways depending upon the structure of the coatings. For crack free coatings the sample configuration shown in Fig. 2 was used. A short length of the coated wire was attached to a polycrystalline alumina plate with platinum paste. Care was taken to ensure that the entire surface of the coating was covered with the paste. A second platinum

lead wire was attached to the platinum paste and the entire assembly was cured at 1200°C. The core wire and the second lead were attached to a Hewlett Packard multimeter and the resistance of the coating was measured as a function of temperature in the interval 800-1050°C. The temperature was raised in 50°C increments and the sample was held at each temperature for 20-30 minutes to allow the temperature to stabilize. The resistance values were recorded on a computer. A resistance reading was taken every two seconds until 200 values had been accumulated. The average and standard deviations for each set of readings were calculated. These values were later converted to resistivity using the equation  $\rho = (R2\pi l(r_0 + t/2))/t$  where  $R$  is the measured resistance,  $r_0$  is the radius of the uncoated wire,  $t$  is the coating thickness, and  $l$  is the length of the coated wire covered by platinum paste. Depending upon sample temperature, the measured resistance values ranged from 0.66 M $\Omega$  at 1050°C to 9.60 M $\Omega$  at 800°C. The standard deviations were consistently about 30% of the average readings.

The cracked EPD coatings could not be measured by the method used for crack free coatings because the Pt paste entered the cracks and made contact with the wire. To measure the resistance of these coatings, the

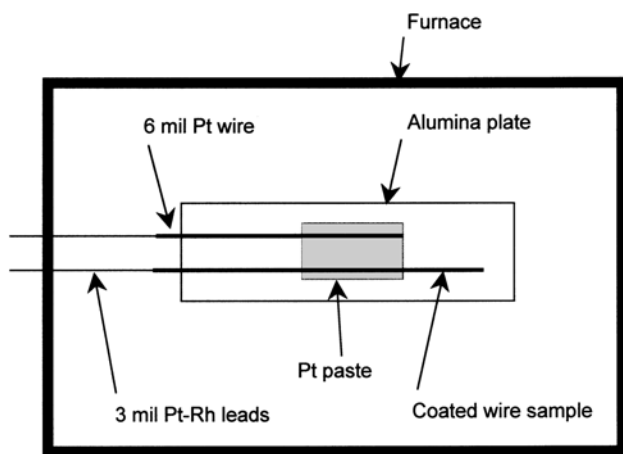


Fig. 2. Sample configuration for measuring resistivity of slurry coated samples.

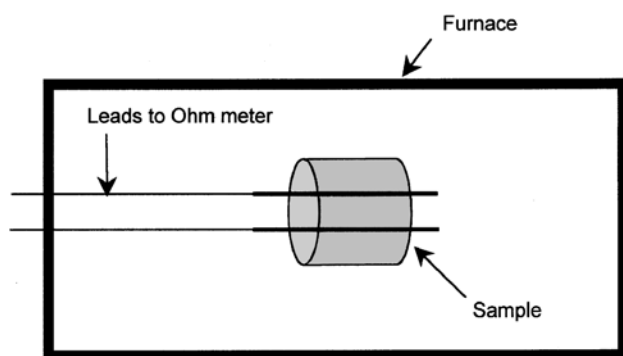


Fig. 3. Sample configuration for resistivity measurements on EPD samples.

configuration shown in Fig. 3 was used. A “hairpin” shaped piece of Pt wire, having a known distance between the legs was EPD coated and sintered. The bend in the hairpin was then cut away and the resistance of the coating, remaining between the legs, was measured with a Keithley electrometer (model 6517). The sample was held 30 min at each temperature before a reading was taken. The resistance was not stable and the most frequently observed values were recorded. Measured resistance ranged from 10 M $\Omega$  at 1050°C to 222 M $\Omega$  at 900°C. The resistivity of the coatings was calculated using the approximation  $\rho = Rd_0t/l$  where  $R$  is the measured resistance,  $d_0$  is the diameter of the uncoated wire,  $l$  is the length of the coating, and  $t$  is the separation between the two wires.

## Results and Discussion

### Observations on the coating processes

Although EPD from aqueous suspensions did not produce the best coatings, this method was studied in greater detail than EPD from organic suspensions. The reason for this was that charging of the particles was more easily controlled in aqueous suspensions. The rate of coating deposition was measured at constant currents of 1.0, 2.0, and 3.0 mA in a slurry containing 40 wt.% Al<sub>2</sub>O<sub>3</sub>. As seen in Fig. 4, the deposition rate is constant with time at each current level, as would be expected. However, the rate saturates at about 2.0 mA and does not increase significantly with further increases in current. This behavior is probably related to changes in conditions at the anode, where the particles are deposited. As the current increases, the voltage drop through the suspension increases and since the force on the particles increases, one would expect that the deposition rate would also increase. However, most of the potential drop occurs in a thin sheath about

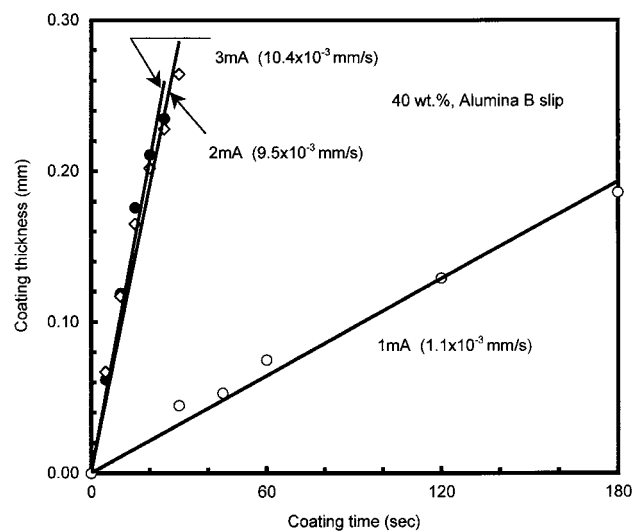


Fig. 4. Coating thickness as a function of deposition time and current. Coating rates are given in parentheses.

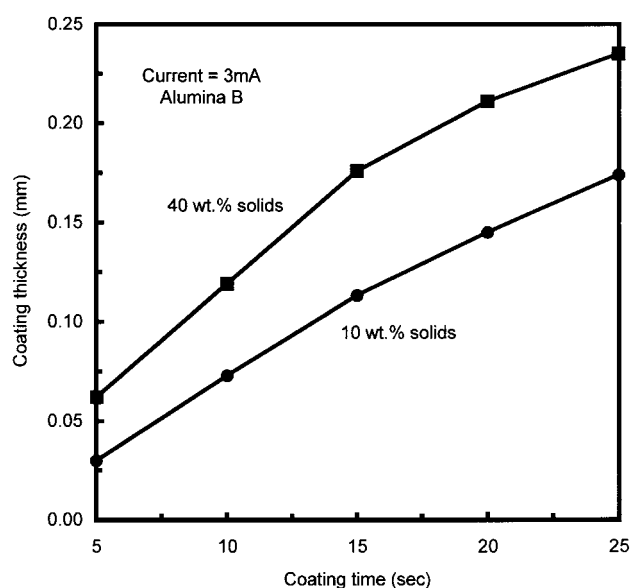


Fig. 5. Effect of solids content on the evolution of coating thickness with time.

the anode, eventually the suspension within this region becomes depleted of alumina particles, and the deposition rate is limited by the diffusion rate of particles to the anode. Under these conditions a greater fraction of the current is carried by the ions in the electrolyte. This means that the rate of electrolysis of water increases, and the anode becomes covered with a layer of oxygen bubbles. The bubble layer restricts access of particles to the surface of the growing deposit and the deposition rate is further slowed. As will be seen, photomicrographs clearly show that gas bubbles locally restrict deposition of alumina particles. Due to these effects, the quality of the coatings was lower at high deposition rates. The coatings produced under these conditions contained large pores and had uneven or "hilly" surfaces. As shown in Fig. 5, the deposition rate increased as the concentration of alumina particles increased. The effect is not linear, and a fourfold increase in alumina concentration leads to only a 36% increase in coating thickness after 25 seconds of deposition.

Since the EPD coatings made from aqueous suspensions were poor in quality, we decided to abandon this approach and to use organic solvents to formulate the suspensions. Organic solvents do not electrolyze and gasses are not produced at the electrodes. As noted earlier, no dispersants or charging agents were added to the slurries based on ethanol-acetone mixtures. Nevertheless, the alumina particles were sufficiently charged to undergo electrophoretic deposition. The conductivity of the ethanol-based suspensions was measured as the solids content increased. The data in Fig. 6 show that the conductivity is linearly related to the alumina concentration. Sarkar and Nicholson [3] have proposed a mechanism for the charging of  $\text{Al}_2\text{O}_3$  in ethanol. The

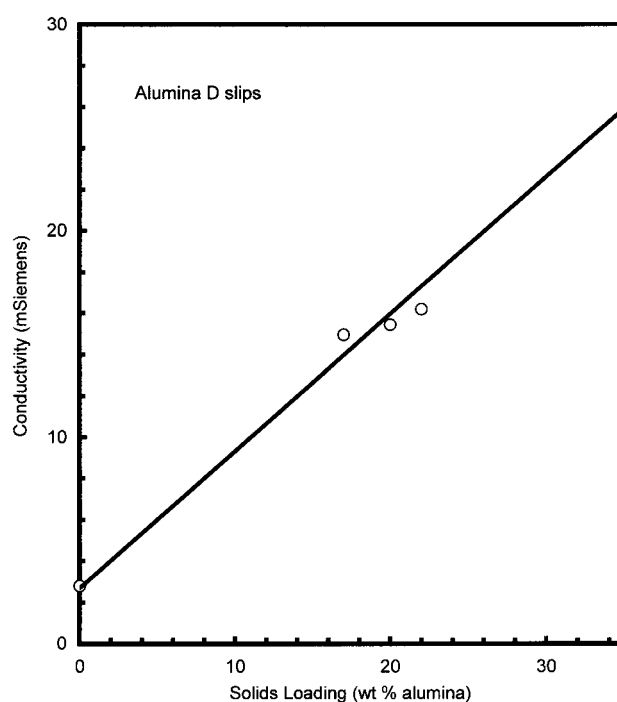
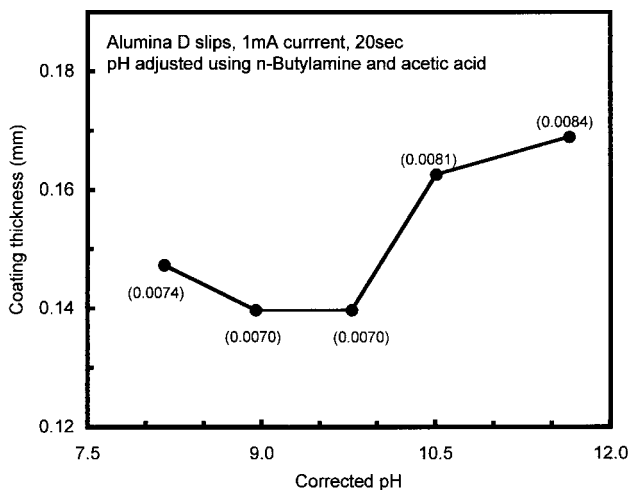


Fig. 6. Conductivity of slips with various loadings of alumina dispersed in a mixed ethanol-acetone solvent.

first step is the adsorption of ethanol molecules at basic surface sites. The adsorbed molecules then dissociate into protons and  $\text{C}_2\text{H}_5\text{O}^-$  ions. The  $\text{C}_2\text{H}_5\text{O}^-$  ions dissolve into the liquid phase and the protons remain adsorbed on the alumina surface. The alumina particles therefore acquire a positive charge and the solvent becomes more conductive due to the higher concentration of  $\text{C}_2\text{H}_5\text{O}^-$  ions. This charging mechanism explains the conductivity seen in Fig. 6 and the fact that the alumina particles are deposited at the cathode.

An attempt was made to control the dispersion of alumina particles in ethanol suspensions by changing the pH. The pH was adjusted by adding small quantities of glacial acetic acid or n-butylamine. The pH of the suspensions was measured as well as the thickness of coatings deposited in 25 seconds at a current of 1.0 mA. The pH readings were corrected for the non aqueous environment by the method in reference 3. The data are shown in Fig. 7. Increasing the pH had a small effect on the coating rate under these conditions. What is more important is that the coating rate overall is faster ( $\sim 7.6 \times 10^{-3}$  mm/s) than that under similar conditions in an aqueous system ( $9.6 \times 10^{-4}$  mm/s, Fig. 4). This is important because it shows that deposition of alumina from ethanol-acetone mixtures is a rapid process.

The ethanol-based slips were not very stable, the alumina settled rapidly but the resulting sediments were easily re-dispersed. These are characteristics of partially flocculated suspensions. Flocculation occurs when the particle charge is small and the repulsive energy barrier between approaching particles is small.



**Fig. 7.** Effect of pH on non-aqueous EPD coating thickness. Coating rates (mm/s) are given in parentheses.

This same energy barrier must be surmounted when particles deposit on the cathode. We believe that the low energy barrier is the reason for rapid deposition in this system.

Slurry coating was studied as an alternative method for applying alumina directly onto platinum wires. The viscosity of the slurry and the speed of the wire through the slurry determine the structure and thickness of the coating. If the viscosity was too low, the coating broke up and became a “string of beads” on the wire. This was caused by Rayleigh instability, the same phenomenon responsible for the break up of a falling stream of water into spherical droplets. The beads were spaced about four diameters apart and left too much exposed wire to be useful for electrical insulation. On the other hand, if the viscosity was too high or if the speed of the wire was too high, the coatings were too

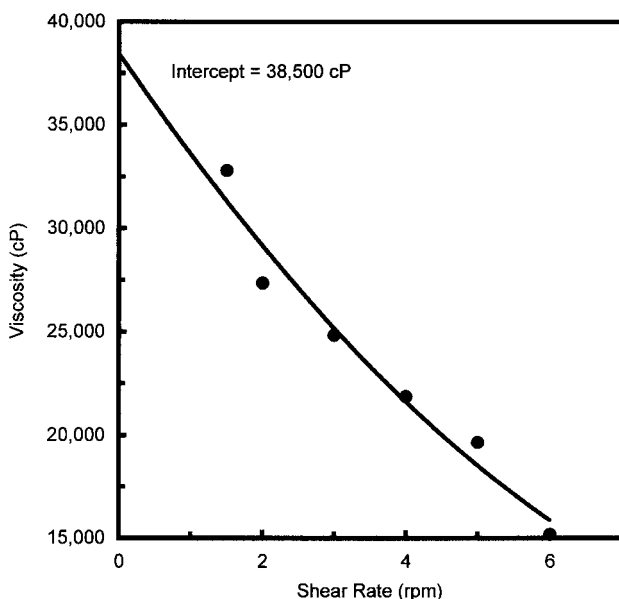


**Fig. 8.** Viscosity of suspension used for slurry coating.

thick and too uneven to be useful. With the slurry in Table 2, smooth cylindrical coatings about 0.6 mil thick were made when the wire speed was 0.5 cm/s. This slurry produced the best results of any tried, and as Fig. 8 shows it was thixotropic, having shear-thinning behavior. As the wire was drawn through the slurry, the liquid near the wire was sheared, the viscosity in the sheared zone decreased, and a thin smooth layer of suspension coated the wire. Shortly after leaving the bath, the shearing of the liquid stopped and the viscosity increased due to the thixotropic effect. In addition, solvent evaporation occurred and this also contributed to an increase in viscosity of the suspension adhering to the wire. If the viscosity increased rapidly enough, the coating set up before Rayleigh instability could cause it to break up into a string of beads.

### Structure of the coatings

The structure of a typical dried coating produced by EPD from an aqueous slurry is shown in Fig. 9. The coating contains “craters” where it grew around oxygen bubbles attached to the anode surface. When the bubbles break away, the coating tends to fill in the craters but this process is often incomplete and the surface of the coating has irregular undulations which are relicts of the incompletely filled craters. We believe that the large-scale variations in coating diameter, seen in Fig. 9, are caused by this process. The wet coatings are free of cracks, and this indicates that the cracks seen in Fig. 9 are caused by drying shrinkage of the constrained coating. All of the defects seen in Fig. 9 remain in the coating after the wire has been sintered. The drying cracks become wider during sintering due to firing shrinkage. The spacing of the cracks is fairly regular over the length of the coated wire. Detailed studies [4], not reported here, indicate that the crack spacing is influenced by the wire diameter, coating thickness, wire type, and surface roughness of the wire. If the coating is thin, a more complex system of cracks develops as shown in Fig. 10. The cracking pattern shown in Fig. 10 is undesirable since the coating flakes of the wire when it is bent around corners. As will be

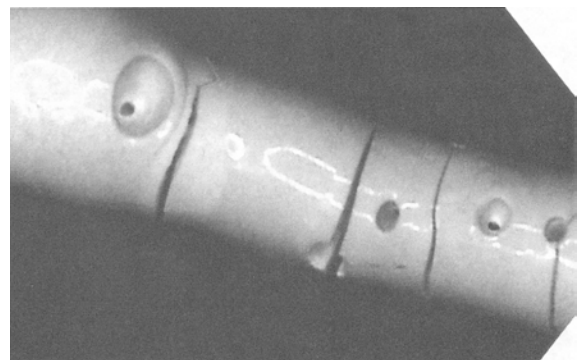


**Fig. 9.** An EPD coating made from an aqueous slip. The large pores formed as the coating grew around oxygen bubbles attached to the electrode. The bubbles were formed by electrolysis of water.

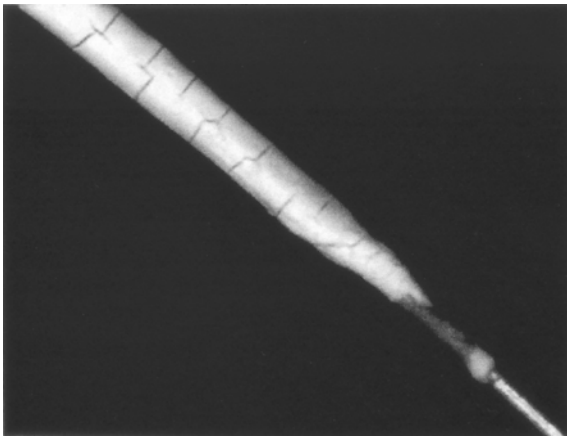


**Fig. 10.** Optical micrograph of an aqueous EPD coating showing an undesirable interconnected cracking pattern.

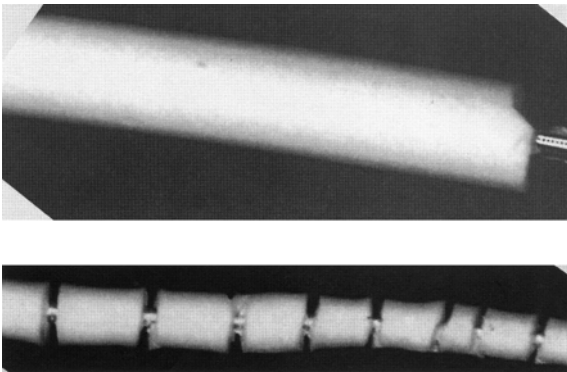


**Fig. 11.** Coatings prepared by EPD from ethanol-based dispersions. No cracks were present after drying but transverse cracks developed during sintering. Wire diameter=5.8 mil.

shown later, the regular transverse cracks (Fig. 9) may be useful since they prevent coating loss when the wire is bent.

The coatings produced by EPD from alcohol-based suspensions behave differently than those made from aqueous suspensions. Figure 11 shows that the coatings can be dried without cracking, but when sintered, these coatings develop regularly spaced cracks similar to those found in aqueous EPD coatings. Chiu, Garino and Cima [5, 6] have analyzed the stresses developed during drying of constrained ceramic films. Their analysis indicates that the drying stress in a constrained coating is due to surface tension forces. Since acetone and ethanol have only 1/3 the surface tension of water, the drying stresses in alcohol-acetone based EPD coatings are apparently too low to cause cracking as the coating dries. Furthermore, since no gas bubbles were evolved during the coating process, the coatings had smooth cylindrical surfaces of constant diameter. The dimensions of the coating before and after sintering were used to calculate the radial and longitudinal firing shrinkage. The radial firing shrinkage was 33% and the longitudinal firing shrinkage was 16%. The volume shrinkage on firing was 54%, which is rather large and

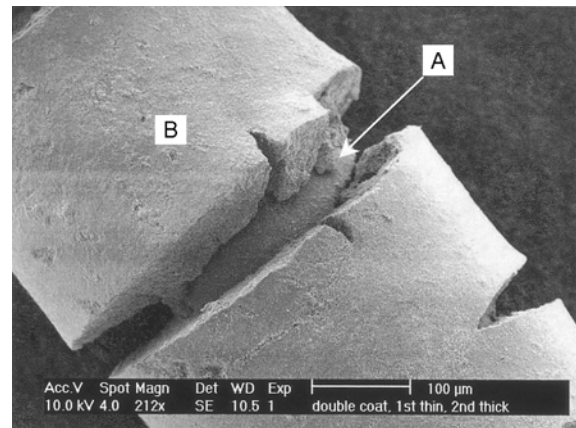


**Fig. 12.** Scanning electron micrograph showing a second coating covering the cracks in the first coating in a double EPD-coated wire. A=first coating (thickness=1.7 mil), B=second coating (thickness=2.8 mil).

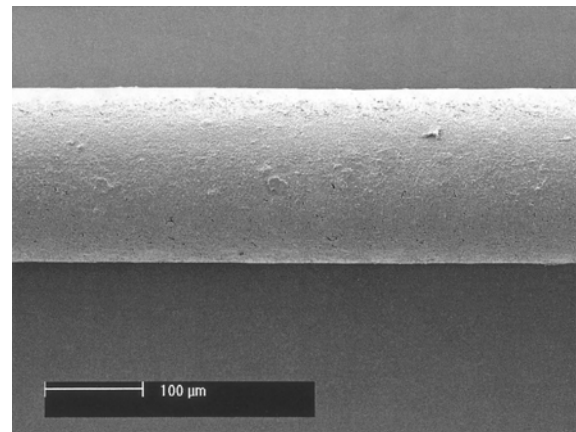


**Fig. 13.** Scanning electron micrograph of a sintered slurry coated wire, showing a smooth crack free surface. Wire diameter=5.8 mil.

indicates that the dried coatings had a packing fraction of only 0.46. This is consistent with the earlier observation that the alumina-ethanol-acetone suspensions were flocculated.

The cracks in a sintered coating can be filled by a second EPD coating as shown in Fig. 12. However, the second coating develops a new set of cracks, which are located over the intact regions of the first coating. Apparently, the initial cracks serve as "anchoring points" for the second coating. As the second coating shrinks during sintering, new cracks develop between these anchor points. In any case, no exposed metal wire is visible through these double coatings.

The structure of a sintered, slurry coated specimen is shown in Fig. 13. The coating has a smooth surface and is free of cracks. The thickness of the coating was 0.61 mil. The same specimen is shown at higher magnification in Fig. 14. The micrograph shows that the coating was sintered to theoretical density since it is free of porosity. The fine structure within individual grains was caused by

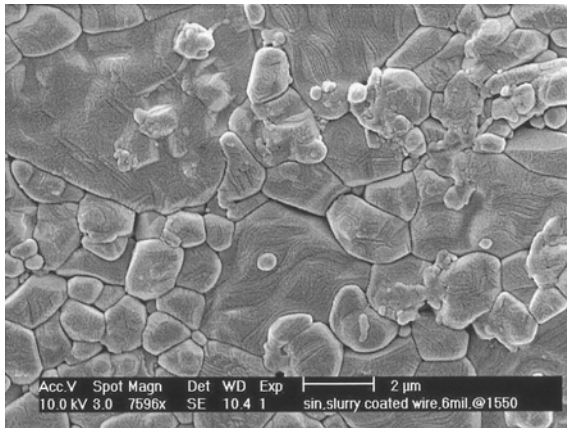


**Fig. 14.** SEM micrograph of a sintered, slurry coated, sample showing that the alumina coatings were sintered to theoretical density.

thermal faceting of high energy surfaces on the particles, and is often observed in alumina after sintering at high temperatures. The microstructure in Fig. 14 was also observed in sintered coatings made by EPD from both alcohol and water based suspensions.

#### Coating adherence

Wires must be bent around sharp corners when installed in an engine. Since all ceramics are brittle, they crack when bent. However if the cracks are small and if the alumina coating adheres very strongly to the wire, the coating will remain in place after cracking and continue to provide electrical insulation. To qualitatively assess coating adherence, we bent sintered wires 360° around 1/16 inch drill rod and then examined them under a microscope. Figure 15 shows what happens when a pre-cracked coating is bent. The wire, bridging the cracks, bends and stretches but the wire inside sintered segments of coating remains straight. On the inside radius of the bend, the cracks close while on the outside radius they open up. Since all of the

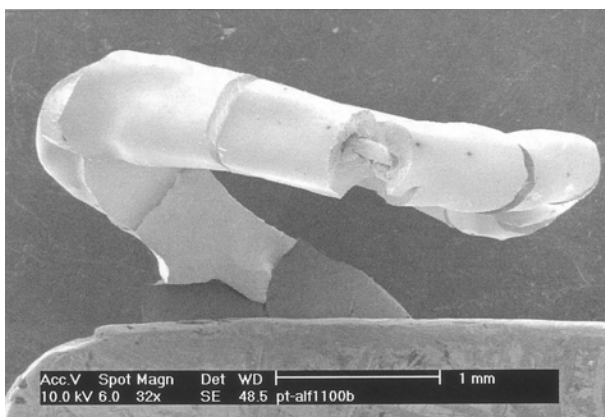


**Fig. 15.** SEM micrograph of a thick, pre-cracked EPD coating showing that the coating remains in place when bent around a 1/16" rod.

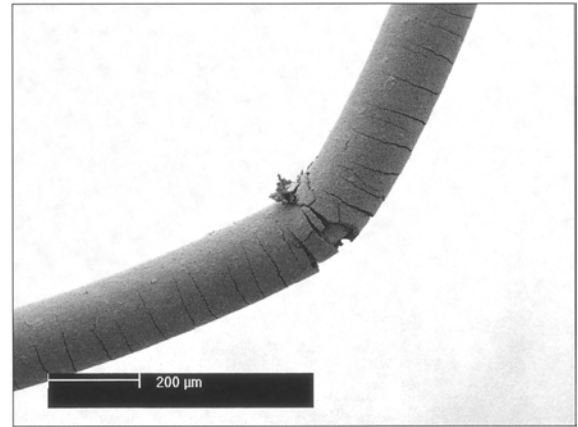


**Fig. 16.** SEM micrograph of a slurry coated sample showing that only a small portion of the coating falls off even at sharp bends.

bending strain occurs within the wire, none of the alumina coating is lost nor are new cracks formed. Because the widest opening of the cracks is only 250 µ (9.8 mil), engine components beneath the wire or adjacent wires are unlikely to make contact with the central conductor. Therefore, although the coatings are cracked, such wires may be useful if the coating can withstand the intense acoustic vibrations found in turbine engines. Future tests are planned to determine how well the coatings will withstand conditions within an operating engine.

The response of a sintered, slurry coated wire to a sharp bend is shown in Fig. 16. The coating develops a series of narrow transverse cracks whose spacing is proportional to the local bend radius. However, very little of the coating spalls off the wire and the coating can still provide electrical insulation. The most severe damage occurs at the apex of the bend, but even here, nearly all of the coating remains attached to the wire. Whether it will continue to remain attached when subjected to intense engine vibrations is an open question, which will be answered in the future by testing bent

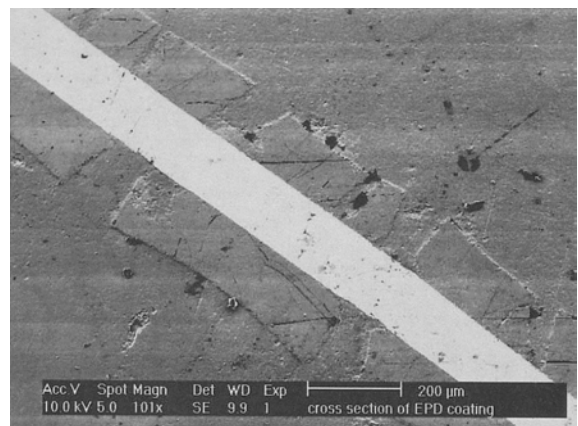


**Fig. 17.** Cross section of a sintered coating made by non-aqueous EPD. The coating was made from a suspension of alumina D and was sintered at 1550°C for 2.5 hr.

wires in an acoustic chamber, which simulates engine vibrations.

A longitudinal section through a sintered, EPD coated wire is shown in Fig. 17, this is the same type of wire shown in Fig. 11. The bright diagonal band is the platinum wire, the coating (including cracks) is the lower brightness region next to the wire, and outside of this (and filling the cracks) is the polymer material used to mount the sample for polishing. The cracks in this coating developed during sintering. The average coating thickness is 4.8 mil and the average crack width is 3-4 mil. The outer edges of the coating segments are bowed away from the central wire. At the ends of the segments the coating has pulled away from the wire leaving small gaps parallel to the Pt-Al<sub>2</sub>O<sub>3</sub> interface. The geometry of the coating segments is an indication that a strong bond exists between the coating and the platinum wire. The frictional forces at the central portions of the segments were sufficiently large to prevent shrinkage of the alumina next to the interface. However, the outer surfaces of the segments were unconstrained and shrank. As a result, the outer surface of the coating was in tension and the part next to the wire was in compression. Eventually these stresses increased to the point where they exceeded the tensile strength of the Pt-Al<sub>2</sub>O<sub>3</sub> bond. The bond then ruptured, gaps opened along the interface, and the ends of the coating bowed outward by plastic flow. Despite the gaps, most of the interface remained strongly bonded and the alumina segments were held firmly to the wire.

### Wire flexibility

The minimum bend radius of a wire having a pre-cracked coating can be estimated based upon the following criteria. To prevent damage to the platinum wire, its centerline fiber must remain at constant length, that is the wire should not be stretched. To prevent additional cracks and coating loss, bending should cease when the edges of the cracks come into contact with each other. The geometry for this situation is shown in Fig. 18. The bend angle ( $\theta$ ) which can be accommodated at each Crack is  $\tan(\theta/2) = w/(2(t + r_o))$  where  $w$  = the average crack width before bending,  $t$  = the coating thickness, and  $r_o$  = the radius of the uncoated wire. The number of segments ( $n$ ) needed to bend the wire in a circle can be calculated from  $n = 360/\theta$ , and therefore the circumference ( $C$ ) of the circle at the centerline of the wire is  $C = nL_s$  where  $L_s$  is the average distance between cracks, measured at the crack centers. The radius ( $r_c$ ) of the circle at the centerline of the wire is given by  $r_c = C/2\pi$  and the minimum radius ( $r_{min}$ ) at the inside edge of the coating is  $r_{min} = r_c - t$ . The minimum bend radius for the wire shown in Figs. 11 and 17 was estimated to be 0.044". In other words, the wire could be bent around a corner, having this radius, without creating new cracks or stretching the conductor wire. The minimum bend radius can be used as a

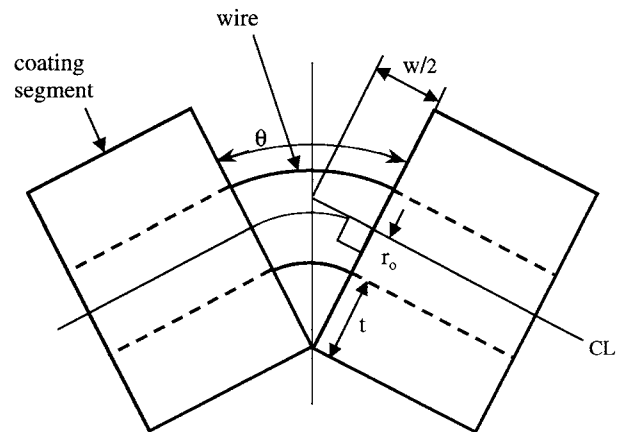


Fig. 18. Geometry around a single bend in a pre-cracked wire. See text for meaning of symbols.

measure of the flexibility of wires having pre-cracked coatings. The flexibility is inversely related to the minimum bend radius.

A similar calculation cannot be done for wires having continuous, crack free, coatings since there are no pre-existing cracks. However, since the coatings are thin, they offer little resistance to bending and the slurry coated wires, in this sense, are quite flexible. A more practical criterion, which cannot be evaluated at pre-sent, is how small the bend radius can be without resulting in excessive damage to the coating.

### Coating resistivity

The high temperature resistivity of typical coatings is summarized in Table 3. The measured resistances (and dimensions) of the coatings are included in the table to show that the resistance values themselves are in the Mega Ohm range at temperatures up to 1050°C. Both the slurry coatings and the alcohol-based EPD coatings have high temperature resistivities, which greatly exceed the PIWG target of  $1 \times 10^6 \Omega\text{-cm}$  at 800°C. Hence in terms of resistivity alone, either type of coating will be useful in modern turbine engines. The resistivity of a pure, sapphire single crystal [7] is shown in Table 3 for comparison to our coatings. Our coatings do not approach the ultimate resistivity of alumina. There are several potential reasons for this, but the most likely explanation is that our values are dominated by surface resistivity, since we took no special precautions to clean the coatings prior to making measurements. In addition, the platinum paste contains impurities (oxides) to improve its adherence, and we did not use guard rings to intercept and eliminate the contribution of surface currents to our measured resistance values. Moulson and Popper [7] have shown that all of these factors contribute to lowering of measured resistivity. However, since none of these precautions will be taken when wires are installed in engines, our values are indicative of what can be expected in practice.

At 1050°C the resistivity of the slurry coating is

about seven times that of the EPD coating. Figure 19 shows that the resistivity values for the two types of coatings converge at lower temperatures and become equal at  $\sim 850^\circ\text{C}$ . The difference in high temperature resistivity is in part due to the much longer path that surface currents must traverse in slurry coated samples. In the slurry coated samples this path is at least several centimeters long since it includes the entire length of alumina coating not covered by the platinum paste electrode (see Fig. 2). In contrast, the path length for surface currents in an EPD coated the specimen is only 0.055 cm, the separation distance between the two embedded wires (see Fig. 3).

The resistivity values were converted to conductivity and a plot of  $\ln(\sigma)$  versus  $1/T$  was used to extract the activation energies for conduction. For the sapphire single crystal, the EPD coating, and the slurry coating these values were 3.69, 2.8, and 1.4 eV respectively. Since the band gap of alumina is 8.8 eV, all of the samples mentioned are conductive by virtue of impurity states in the band gap or by surface conduction. The higher activation energy for the EPD coating (2.8 eV) compared to the slurry coating (1.4 eV) may be due to impurities in the platinum paste, used to cover a portion of the slurry coated sample. At the curing temperature of the paste ( $1200^\circ\text{C}$ ), these oxide impurities could diffuse into the alumina and introduce additional energy states into the band gap which are more easily populated by thermally excited electrons or holes. The net result would be to reduce the activation energy for conduction.

Despite all the limitations, one can conclude from our measurements that both types of coatings exceed the electrical requirements for use in engines.

## Conclusions

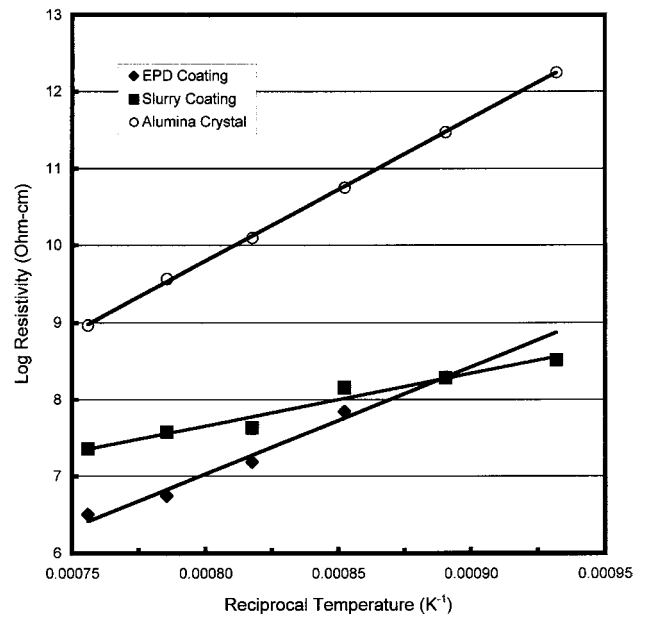


Fig. 19. Comparison of the resistivity of an alumina single crystal with that of alumina coatings made by EPD and slurry coating.

Short lengths of platinum wire were coated with alumina by slurry coating and by electrophoretic deposition from alcohol based suspensions. The coatings were sintered to theoretical density at  $1500\text{--}1600^\circ\text{C}$ . Two types of coatings resulted. One type, prepared by slurry coating, was about 0.6 mil thick and free of cracks and other defects. When bent, this coating fractures but virtually all of the alumina remains attached to the wire. The electrical resistivity of this type of coating was  $3.4 \times 10^8 \Omega\text{-cm}$  at  $800^\circ\text{C}$ . The other type, prepared by electrophoretic deposition, was about 5.0 mil thick and had regularly spaced transverse cracks about 3.0 mil wide. These cracks relieve the stress when the wire is bent, no coating is lost, and no new cracks are

Table 3. Electrical properties of alumina coatings made by EPD and slurry coating

Temperature ( $^\circ\text{C}$ )	EPD coated samples		Slurry coated samples		Resistivity $\text{Al}_2\text{O}_3$ Xtal.* ( $\Omega\text{-cm}$ )
	Resistivity ( $\Omega\text{-cm}$ )	Resistance ( $10^6 \text{ Ohm}$ )	Resistivity ( $\Omega\text{-cm}$ )	Resistance ( $10^6 \text{ Ohm}$ )	
800	—	—	$337 \times 10^6$	9.6 (2.0) <sup>†</sup>	$1.79 \times 10^{12}$
850	—	—	$197 \times 10^6$	5.6 (1.4)	$3.00 \times 10^{11}$
900	$70.1 \times 10^6$	222	$145 \times 10^6$	4.1 (1.3)	$5.70 \times 10^{10}$
950	$15.3 \times 10^6$	48.1	$43.2 \times 10^6$	1.2 (0.4)	$1.26 \times 10^{10}$
1000	$5.53 \times 10^6$	17.5	$38.3 \times 10^6$	1.1 (0.4)	$3.68 \times 10^9$
1050	$3.16 \times 10^6$	10.0	$23.2 \times 10^6$	0.66 (0.3)	$9.22 \times 10^8$
Radius of wire ( $r_0$ )		0.127 mm	—	0.071 mm	—
Thickness of coating (t)		0.55 mm	—	0.022 mm	—
Sample length (l)		6.84 mm	—	15.0 mm	—
Alumina type		D	—	F	—
Total metal oxide impurity		148 ppm	—	177 ppm	—

\*Data are for an alumina single crystal, reference 7.

<sup>†</sup>Numbers in the parentheses are the standard deviations, 200 measurements were made.

formed. The minimum bend radius for such a coating, without damage to the Pt wire, is about 45 mil. The electrical resistivity of this type of coating was  $7.5 \times 10^8 \Omega\text{-cm}$  at  $800^\circ\text{C}$ . These coatings meet or exceed most of the targets set by PIWG for new lead wire technology, to be used in advanced turbine engines. These targets were; good wire flexibility, coating resistivity of  $1.0 \times 10^6 \Omega\text{-cm}$  at  $800^\circ\text{C}$ , low conductor resistance, diameter for a wire pair less than 63 mil, the insulation is not degraded at  $800^\circ\text{C}$ , and joining by soft soldering or spot welding. The coated wires, we have produced, are very flexible and greatly exceed the resistivity requirement on the insulation. The resistivity of pure platinum is low ( $1 \times 10^{-5} \Omega\text{-cm}$  at  $25^\circ\text{C}$ ) and the diameter for a pair of wires is between 14 and 30 mil, depending upon wire type. Alumina is one of the materials most resistant to chemical attack and environmental degradation. The joining of our wires by soldering or spot welding has not been tested, but should be possible once methods are developed for stripping the alumina insulation. Although many of the PIWG targets have been met, there are several questions remaining unanswered. The most important ones are; the resistance of the insulation to dislodgment by the intense acoustical vibrations found in operating engines, and the effect of cracks in the insulation on its electrical resistivity in an engine environment. Tests are planned to answer both of these questions. Finally, the coated wires are sufficiently promising to justify further development of the techniques needed to manufacture them. In particular, pilot scale facilities should be developed which will allow production of long lengths of coated wire.

### Acknowledgements

This material is based upon work supported by the NASA Glenn Research Center Award No. NAG 3-2090. Any opinions, findings, conclusions, or recommendations expressed in this publication are those of the authors and do not necessarily reflect the views of the NASA Glenn Research Center. We thank the Members of the Propulsion Instrumentation Working Group (PIWG) and the Ohio Aerospace Institute for calling our attention to the problem. We particularly thank Dr. Jih-Fen Lei of NASA Glenn for her support and encouragement of this project.

### References

1. A.A. Bauer and J.L. Bates, Battelle Memorial Inst. Report #1930, July 31, 1974.
2. T.E. Faber, Fluid Dynamics For Physicists, 295 Cambridge University Press (1995).
3. P. Sarkar and P.S. Nicholson, "Electrophoretic deposition (EPD): Mechanisms, Kinetics, and Applications to Ceramics", J. Am. Ceram. Soc. 79[8] (1996) 1987-2002.
4. Vidya Praveen Bhallamudi, Coating high temperature lead wires with electrically insulating alumina by electrophoretic deposition and slurry coating, M.S. Thesis, The Ohio State University (2000).
5. R.C. Chiu, T.J. Garino, and M.J. Cima, "Drying of granular ceramic films: I, Effect of processing variables on cracking behavior", J. Am. Ceram. Soc. 76[9] (1993) 2257-2264.
6. R.C. Chiu and M.C. Cima, "Drying of granular ceramic films: II, Drying stress and saturation uniformity", J. Am. Ceram. Soc. 76[11] (1993) 2769-2777.
7. A.J. Moulson and P. Popper, "Problems associated with the measurement of the volume resistivity of insulating ceramics at high temperature", Proceedings Brit. Ceram. Soc. (1968) No. 10, 41-50.